

AperTO - Archivio Istituzionale Open Access dell'Università di Torino

**Photochemical formation of nitrite/nitrous acid (HONO) upon irradiation of nitrophenols in aqueous solution and in viscous secondary organic aerosol proxy**

**This is the author's manuscript**

*Original Citation:*

*Availability:*

This version is available <http://hdl.handle.net/2318/1658093> since 2018-01-19T09:26:34Z

*Published version:*

DOI:10.1021/acs.est.7b01397

*Terms of use:*

Open Access

Anyone can freely access the full text of works made available as "Open Access". Works made available under a Creative Commons license can be used according to the terms and conditions of said license. Use of all other works requires consent of the right holder (author or publisher) if not exempted from copyright protection by the applicable law.

(Article begins on next page)

# **Photochemical formation of nitrite/nitrous acid (HONO) upon irradiation of nitrophenols in aqueous solution and in viscous secondary organic aerosol proxy**

**Francesco Barsotti,<sup>a</sup> Thorsten Bartels-Rausch,<sup>b,\*</sup> Elisa De Laurentiis,<sup>a</sup> Markus Ammann,<sup>b</sup> Marcello Brigante,<sup>c</sup> Gilles Mailhot,<sup>c</sup> Valter Maurino,<sup>a</sup> Claudio Minero,<sup>a</sup> Davide Vione<sup>a,d,\*</sup>**

<sup>a</sup> Università di Torino, Dipartimento di Chimica, Via Pietro Giuria 5, 10125 Torino, Italy.

<sup>b</sup> Paul Scherrer Institute, Laboratory of Environmental Chemistry, 5232 Villigen PSI, Switzerland.

<sup>c</sup> Université Clermont Auvergne, CNRS, Sigma Clermont, Institut de Chimie de Clermont-Ferrand, F-63000 Clermont-Ferrand, France.

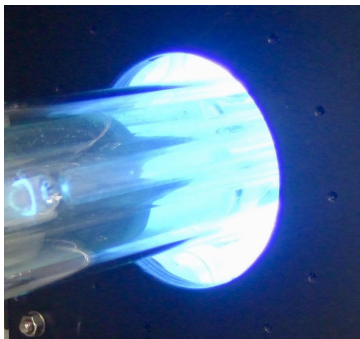
<sup>d</sup> Università di Torino, Centro Interdipartimentale NatRisk, Largo Paolo Braccini 2, 10095 Grugliasco (TO), Italy.

\* Address correspondence to either author: *thorsten.bartels-rausch@psi.ch* (TBR; Phone +41-(0)56-3104301; Fax +41-(0)56-3104435) or *davide.vione@unito.it* (DV; Phone +39-011-6705296; Fax +39-011-6705242).

## ***Abstract***

Irradiated nitrophenols can produce nitrite and HONO in bulk aqueous solutions and in viscous aqueous films, simulating the conditions of a high solute strength aqueous aerosol, with comparable quantum yields in solution and viscous films ( $10^{-5}$ - $10^{-4}$  in the case of 4-nitrophenol), and overall reaction yields up to 0.3 in solution. The process is particularly important for the *para*-nitrophenols, possibly because their less sterically hindered nitro groups can be released more easily as nitrite/HONO. The nitrophenols giving the highest photoproduction rates of nitrite/HONO (most notably, 4-nitrophenol and 2-methyl-4-nitrophenol) could significantly contribute to the occurrence

of nitrite in aqueous phases in contact with the atmosphere. Interestingly, dew water evaporation has shown potential to contribute to the gas-phase HONO levels during the morning, which accounts for the possible importance of the studied process.



## Introduction

The UV photolysis of HONO (reaction 1) is a major source of HO<sup>•</sup> radicals in the troposphere during the early morning and in indoor environments.<sup>1-5</sup>



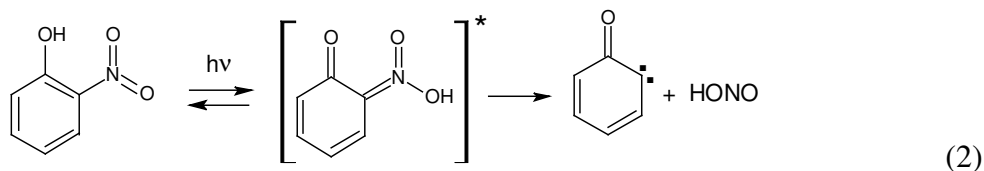
Formation and cycling of atmospheric HO<sup>•</sup>, the main oxidant in the atmosphere, is still under debate.<sup>6</sup> Further, reaction (1) triggers the production of O<sub>3</sub>.<sup>2,7-10</sup>

Atmospheric HONO sources remain unclear, and both gas-phase and heterogeneous sources have been described.<sup>10,11</sup> Debate has arisen as to the nature of the surfaces involved in the heterogeneous process, including the recent identification of humic acids, inorganic oxides and organic films adhering on solid surfaces (urban grime) as likely substrates for HONO formation to take place.<sup>1,12-</sup>

<sup>14</sup> Other potentially important sources of gas-phase HONO are the bacterial processing of soil nitrite<sup>15,16</sup> and the evaporation of nitrite-containing dew or fog water.<sup>17</sup> From this point of view, water droplets act as crucial reservoirs of HONO/NO<sub>2</sub><sup>-</sup> through partitioning/dissolution and

evaporation/emission processes.<sup>18,19</sup> Among the gas-phase HONO sources in the troposphere, the gas-phase photolysis of *ortho*-nitrophenols has been shown to play a potentially important role.<sup>20,21</sup> Nitrophenols are widespread environmental pollutants and their atmospheric occurrence is of particular concern, because their phytotoxic properties have been associated with forest decline.<sup>22,23</sup> Nitrophenols can be emitted as primary pollutants by combustion processes, and they can also be formed by secondary nitration of phenolic precursors.<sup>24-29</sup> Nitrophenols occur in practically all of the atmospheric compartments, ranging from the gas phase (up to hundreds ng m<sup>-3</sup> levels) to the aqueous solutions (concentration levels up to hundreds μg L<sup>-1</sup>) and particles (ng m<sup>-3</sup> levels).<sup>30,31</sup> While 2-nitrophenol is very abundant in the gas phase, the less volatile compounds 4-nitrophenol and 2,4-dinitrophenol are often found in the aqueous phase and on particles (see **Table 1** for structures and acronyms of the studied nitrophenols).<sup>30,32-34</sup>

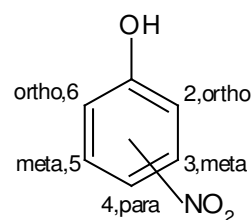
The photolysis of volatile *ortho*-nitrophenols can produce gas-phase HONO, with high efficiencies via an intra-molecular homolytic bond cleavage (reaction 2).<sup>20</sup>



This issue accounts for the interest to investigate a parallel process involving dissolved nitrophenols, also in the light of a recent report that the nitrophenol absorption spectrum is significantly red shifted (and the ability to absorb sunlight consequently enhanced) in condensed phases when compared to the gas phase.<sup>35</sup> In aqueous solution, nitrophenols undergo photoreduction to produce nitroso compounds, but transformation intermediates without N atoms have also been observed.<sup>36,37</sup> The latter compounds suggest that the nitro group could be released under photochemical conditions, but to our knowledge the photoinduced production of nitrite/HONO in solution has received limited attention.

**Table 1.** Structure and naming of nitrophenols studied in this work, as well as their pKa values.<sup>32</sup>

Compound	Acronym	pKa
2-Nitrophenol	2NP	7.2
4-Nitrophenol	4NP	7.1
2,4-Dinitrophenol	24dNP	4.1
2,6-Dinitrophenol	26dNP	4.0
2,6-Dichloro-4-nitrophenol	26dCl4NP	4.0
4-Chloro-2-nitrophenol	4Cl2NP	5.6
3-Methyl-2-nitrophenol	3m2NP	6.6
4-Methyl-2-nitrophenol	4m2NP	7.1
4-Methyl-3-nitrophenol	4m3NP	8.6
2-Methyl-4-nitrophenol	2m4NP	7.4



Moreover, several previous studies have investigated the photochemistry of aqueous nitrophenols under UVC irradiation that is not environmentally significant. UVC radiation can in fact excite different absorption bands compared to sunlight and would often cause photoionisation,<sup>38</sup> a pathway that is usually not followed by phenolic compounds when excited at longer wavelengths.<sup>39</sup>

Interestingly, small molecules such as H<sub>2</sub>O<sub>2</sub>, NO<sub>3</sub><sup>-</sup> and HONO/NO<sub>2</sub><sup>-</sup> can have comparable photolysis quantum yields in aqueous solutions and in viscous or frozen systems.<sup>40,41</sup> A likely reason is that simple structures tend to follow one or few reaction pathways upon photon absorption. In contrast, more complex molecules could undergo multiple photoreaction pathways,

the relative ratios of which might be influenced by the surrounding matrix. Recently, Lignell and coworkers have shown that the photochemistry of 24dNP changes significantly when switching from an aqueous to an organic environment (such as octanol or condensed phase alpha-pinene oxidation products), as typically found in secondary organic aerosol.<sup>42</sup> A significant impact of viscosity/aerosol matrix on heterogeneous reaction rates and photolysis quantum yields of some nitrophenols has been reported.<sup>42</sup> Such shifts in reaction mechanism are also discussed in frozen media for complex reaction systems.<sup>40,43</sup> In an aqueous solution, molecules are surrounded by a water cage and photofragments can undergo cage recombination processes or diffuse into the solution bulk.<sup>44</sup> The geminate cage recombination is favoured in viscous/frozen systems,<sup>45</sup> often inhibiting the direct photolysis processes and modifying the photoreaction kinetics and pathways in different solvents.

The main goal of the present paper is to fill the existing knowledge gaps, by providing an assessment of the nitrite/HONO formation potential upon irradiation of several nitrophenol isomers in aqueous solution and in more viscous films. In the case of the aqueous solutions, the primary photochemical steps that involve light-excited nitrophenols were also investigated by use of the laser flash photolysis technique. Concentration values of substrates and products were measured by liquid chromatography, to avoid possible biases that might arise when using e.g. UV-vis spectroscopy.<sup>42</sup> In the latter case, the photochemical formation of light-absorbing compounds could lead to an underestimation of the nitrophenol transformation rates and, therefore, of the photolysis quantum yields.

## Experimental Section

In this study the production of nitrite and HONO under UV-irradiation was studied in two different matrixes using two specific experimental set-ups, employing in both cases irradiation at  $\lambda > 300$  nm. Low-pH conditions (pH~3, representative of acidic aerosols) were used to ensure the occurrence of the protonated forms of the nitrophenols. High-pH conditions (pH~10) were used to study the behaviour of the deprotonated forms.<sup>46</sup> Irradiation was also carried out at the unmodified solution pH (5-6 depending on the substrate). The latter conditions are representative of pH values that are common in the atmospheric aqueous phase.<sup>47</sup> The rationale for studying the formation of HONO/NO<sub>2</sub><sup>-</sup> in a wider pH range than is justified by the mere atmospheric significance (see the extension to basic conditions) was to get insight into the reactivity of both the undissociated phenols and the corresponding phenolates, which can occur to a variable degree in atmospheric waters. The choice of the single nitrophenols was based on atmospheric occurrence and/or the presence of different substituents on the aromatic ring.

**Irradiation experiments in aqueous solution (simulated sunlight/Solarbox).** Nitrophenol solutions (5 mL total volume) were placed in cylindrical Pyrex glass cells (4.0 cm diameter, 2.5 cm height) and irradiated under magnetic stirring in a solar simulator (Solarbox, CO.FO.ME.GRA., Milan, Italy), equipped with a 1500 W xenon lamp and a 310 nm cut-off filter. The cells were irradiated mainly from the top. The system was cooled by forced air circulation and the temperature of the irradiated solutions was ~30°C. The UV irradiance on top of the solutions (290-400 nm) was  $30.3 \pm 1.1 \text{ W m}^{-2}$ , measured with a CO.FO.ME.GRA. irradiance meter. The spectrum of the filtered lamp was measured with an Ocean Optics USB 2000 CCD spectrophotometer, calibrated with an Ocean Optics DH-2000-CAL source, and normalised to the results of ferrioxalate actinometry.<sup>34,44</sup> Actinometric measures are important to assess how radiation is absorbed in the solution volume

within the reactor, so that radiation absorption can be expressed in the same volume units as the reaction rates, which allows easy calculation of the photolysis quantum yields. **Figure 1** reports as an example the absorption spectrum of 4NP at different pH values and the emission spectrum of the solar simulator. The absorption spectra of the other studied nitrophenols are reported as Supporting Information (hereafter SI).

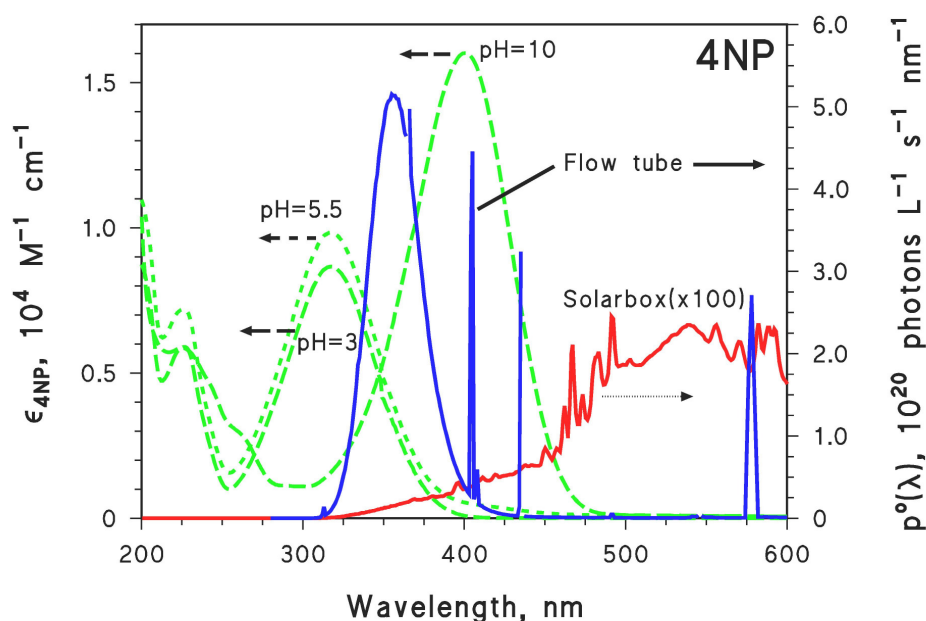
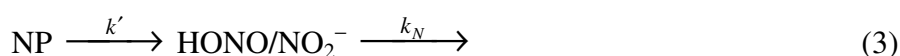


**Figure 1.** Absorption spectra (molar absorption coefficients  $\epsilon$ ) of 4NP at different pH values. Emission spectrum (spectral photon flux density  $p^\circ(\lambda)$ ) of the solar simulator (Solarbox) and of the lamps used to illuminate the flow tube. Note that the Solarbox spectrum was multiplied by a factor of 100 to allow it be plotted against the same scale as the flow-tube lamp.

After the scheduled irradiation times (varied from 1 h to 24 h), the cells were withdrawn from the lamp and the aqueous solutions were analysed by High Performance Liquid Chromatography coupled with UV-Vis detection (HPLC-UV). The HPLC-UV instrument was used to monitor the nitrophenols as well as nitrite + HONO, the latter upon pre-column derivatisation.<sup>48</sup> The detailed

HPLC-UV conditions are reported as SI. Note that the derivatisation reaction requires strongly acidic conditions, thus any nitrite occurring in the sample would be protonated to HONO and quantified as such. Absorption spectra were taken with a Varian Cary 100 Scan double-beam UV-Vis spectrophotometer, using Hellma quartz cuvettes (optical path length 1 cm). The solution pH was measured with a combined glass electrode connected to a Metrohm 713 pH-meter.

The time evolution of the nitrophenols (NP) was fitted with pseudo-first order equations of the form  $[NP]_t = [NP]_o e^{-kt}$ , where  $[NP]_t$  is the nitrophenol concentration at the irradiation time  $t$ ,  $[NP]_o$  the initial concentration (0.1 mM), and  $k$  the pseudo-first order transformation rate constant. The corresponding initial transformation rate was expressed as  $R_o = k [NP]_o$ . NP irradiation causes production of HONO/NO<sub>2</sub><sup>-</sup>, which can in turn be transformed (mainly to nitrate and, to a lesser extent, NO)<sup>49</sup> according to the following consecutive reaction steps:



Under the reasonable hypothesis that HONO/NO<sub>2</sub><sup>-</sup> is formed and transformed with pseudo-first order kinetics, the relevant time evolution can be fitted with the following equation:

$$[N(III)]_t = \frac{k'[NP]_o}{k - k_N} (e^{-k_N t} - e^{-k t}) + [N(III)]_o e^{-k_N t} \quad (4)$$

where  $[NP]_o$  and  $k$  are as above,  $[N(III)]_t$  is the concentration of nitrite + HONO at the time  $t$ ,  $[N(III)]_o$  the initial concentration (some nitrite at low concentration was present as impurity in a few nitrophenol samples), and  $k'$  and  $k_N$  the pseudo-first order rate constants of, respectively, formation and transformation of nitrite + HONO. The initial formation rate of nitrite + HONO ( $R_{NO_2^-+HONO}$ ) was calculated as the slope of the  $[N(III)]_t$  vs.  $t$  curve at  $t = 0$ . The error bounds associated to the initial rates ( $\pm\sigma$ ) were determined from the fit of the experimental data. The rate reproducibility in repeated runs was in the order of 10-15%.

The photodegradation quantum yields of nitrophenols were determined as  $\phi_{NP} = R_o (P_a^{NP})^{-1}$ , where  $P_a^{NP}$  is the photon flux absorbed by the relevant nitrophenol.  $P_a^{NP}$  was calculated as follows:

$$P_a^{NP} = \int_{\lambda} p^{\circ}(\lambda) [1 - 10^{-\varepsilon_{NP}(\lambda) b [NP]}] d\lambda \quad (5)$$

where  $p^{\circ}(\lambda)$  is the incident spectral photon flux density of the solar simulator (see **Figure 1**),  $\varepsilon_{NP}(\lambda)$  the molar absorption coefficient of the nitrophenol at the pH value of the irradiation experiment,  $b = 0.4$  cm the optical path length of the irradiated solution, and  $[NP] = 0.1$  mM the nitrophenol initial concentration. The formation quantum yields of nitrite + HONO were determined as  $\phi_{NO_2^-+HONO} = R_{NO_2^-+HONO} (P_a^{NP})^{-1}$ , where the different quantities are as above. Finally, the formation yield of nitrite + HONO upon nitrophenol photodegradation was calculated as  $\omega_{NO_2^-+HONO} = \phi_{NO_2^-+HONO} (\phi_{NP})^{-1}$ . The described kinetic treatment could be applied to all investigated nitrophenols except for 26dNP, which did not follow a first-order kinetics.

**Flow tube irradiation experiments in citric acid-containing films.** A flow tube served as photo-reactor with a stationary liquid sample, flushed with a stream of humidified N<sub>2</sub> at ~74% relative humidity (294 K). The humidity of the carrier gas was set in a homebuilt humidifier by passing the gas through a Gore-Tex membrane tube immersed in a thermostated water bath. The feeding line was made of a (perfluoroalkoxy) fluoropolymer tubing of 6 mm outer diameter. A gas flow of 1065 mL min<sup>-1</sup> (at norm temperature and pressure) through the photo-reactor was set by a 2 L min<sup>-1</sup> red-y flow regulator (Vögtlin Instruments, Switzerland), with a precision of 1% of the end value. Relative humidity was measured with a dew-point sensor (Meltec UFT 75-AT, Germany) at the exit and entrance of the flow reactor. Nitrogen was of 99.9995% quality. For each experiment, a solution of 0.1 mM 4-nitrophenol (4NP) was prepared in 3 M aqueous citric acid. For some

experiments, 1 M NaOH was added until the pH was set at 3 or 7, respectively. Aliquots of 275  $\mu\text{L}$  of that viscous solution were dosed into the coated wall flow tube and dispersed at its inner wall. A Duran glass tube, 40 cm in length and with an inner diameter of 0.8 cm, served as coated wall flow tube. The glass tube was cleaned by etching with 5 % HF in water and by rinsing with water prior to introducing the 4NP solution, so as to form a thin, homogenous film.<sup>50</sup> The film was dried while rotating the tube in a flow of dry  $\text{N}_2$  at room temperature, until it reached a viscosity at which it would not noticeably run down from the flow tube walls. Then the flow tube was placed in the cooling jacket and exposed to the carrier gas with a relative humidity of 74% at 21°C.

Once the flow tube was attached to the feeding line, the film was allowed to adapt to the temperature of the cooling jacket (21°C) and to establish equilibrium with the relative humidity of the carrier gas. At a fixed relative humidity, the exact concentration of citric acid solutions is determined by the fact that the water activity, i.e., the water vapour pressure above the solution matches the water partial pressure of the carrier gas. Thus, the relative humidity was used in these experiments to set the concentration and thus the viscosity of the citric acid films, which served as matrix to hold the 4NP. Apart from viscosity, the citric acid matrix is expected to be inert and, for instance, no changes in the 4NP absorption spectrum were observed in the presence of citric acid compared to aqueous solutions of equal pH.

The films in the coated wall flow tube were irradiated by 7 fluorescence lamps (UV-A range, Philips Cleo Effect 22 W, 300-420 nm, 41 cm, 2.6 cm o.d.) in a circular arrangement of 10 cm diameter in a homebuilt housing. The light had to pass the Duran glass serving as coated wall flow tube, as well as the water-filled cooling jacket made of Duran glass. The absorption of the water cooling jacket and the Duran glass was measured with a Varian Cary 50 UV/VIS single beam spectrometer. The spectral irradiance in the photo-reactor was measured with a LI-COR 1800 hemispherical, cosine corrected spectro-radiometer.<sup>51</sup> From spectral irradiance, the spectral photon flux density was determined by considering irradiation geometry and film volume (see **Figure 1**).

The volatile photoproduct HONO was emitted to the carrier gas from the irradiated film, quickly removed from the photo-reactor in the carrier gas and quantified in a specific, commercially available instrument. The operation of this instrument (Lopap) has been described before.<sup>52-54</sup> HONO was chemically collected in a stripping coil and converted by the Griess reaction into a dye. The dye concentration was measured in a long path absorption cell. The instrument had a detection limit of 5 ppt and a total accuracy of 10% with an actual time resolution of 3 min under the employed operation conditions. In the experiment described here, only the signal from the first measurement channel of the Lopap instrument was used. The signal was not corrected for potential interferences, which are anyway not expected to introduce an important bias. For instance, if  $\bullet\text{NO}_2$  were initially formed in our system, it would quickly undergo hydrolysis in solution or reaction with 4NP to produce HONO.<sup>30</sup>

**Laser flash photolysis experiments.** Flash photolysis excitation of nitrophenol solutions was carried out using the third harmonic (355 nm) of a Quanta Ray GCR 130-01 Nd:YAG laser system instrument, with a single-pulse energy of 35 mJ. The laser apparatus has been previously described.<sup>55</sup> A 3 mL volume of nitrophenol solution was placed in a quartz cuvette (pathlength of 1 cm) and used for a maximum of four consecutive laser shots to avoid possible interferences by degradation products. Stock solutions of nitrophenols were prepared in Milli-Q water and diluted just before each experiment, in order to obtain the desired concentration. The pH was set using  $\text{HClO}_4$  or  $\text{NaOH}$ . The first-order decay constants were determined from the linear fit of the logarithmic decay of the transient absorbance *vs.* time.

**Reagents and materials.** All the used reagents were at least of analytical grade and were used as received, without further purification. Water used was of Milli-Q quality.

## Results and Discussion

### *Formation of nitrite/nitrous acid upon irradiation of nitrophenols in aqueous solution under simulated sunlight (Solarbox)*

These experiments involved different nitrophenols in a range of pH conditions. The acid-base equilibria allow the occurrence of different species (undissociated nitrophenols and nitrophenolates) that absorb radiation in different spectral intervals (see e.g. **Figure 1**) and have different photolysis quantum yields. Therefore, the rates and quantum yields of both nitrophenol degradation and HONO/NO<sub>2</sub><sup>-</sup> formation are all expected to vary with pH.

**Figure 2a** shows the initial formation rates of nitrite + HONO for the studied nitrophenols at the different pH values, upon irradiation under simulated sunlight. For some nitrophenols (2NP, 4NP, 24dNP, 4Cl2NP and 4m3NP) the formation of nitrite was highest under basic conditions (photolysis of the nitrophenolates), while it was not the case for the other compounds. In the case of 2m4NP and 4m2NP, no nitrite formation was detected at pH~10. Overall, it appears that the *para* nitrophenols caused faster production of HONO/NO<sub>2</sub><sup>-</sup> than other nitroisomers. This was the case of 4NP with respect to 2NP at all pH values. Among the methylnitrophenols, the *para* one (2m4NP) also showed the highest formation rates, except for pH~10. A similar issue holds for the chloronitroderivatives, for which the formation rates were again highest for the *para* nitroisomer (26dCl4NP).

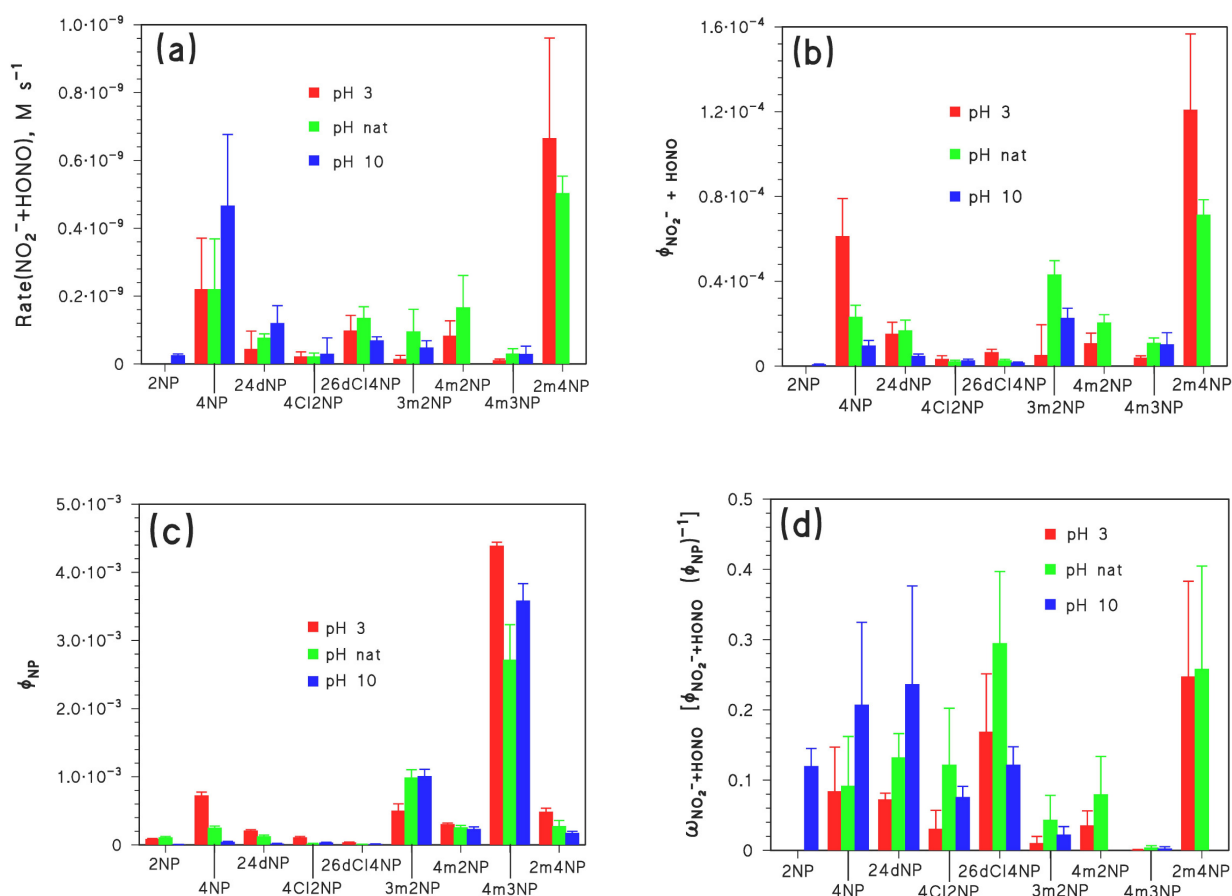


**Figure 2.** Overview of nitrophenol irradiation (0.1 mM initial concentration) under simulated sunlight. (a) Formation rates of nitrite+HONO. (b) Formation quantum yields of nitrite+HONO. (c) Direct photolysis quantum yields of the nitrophenols. (d) Formation yields of nitrite+HONO from the nitrophenols (ratios between the quantum yields of nitrite+HONO formation and the quantum yields of nitrophenol photodegradation). The solution pH was either unadjusted (nat, i.e. pH = 5 to 6), or adjusted with HClO<sub>4</sub> (pH~3) or NaOH (pH~10). The error bars represent  $\pm\sigma$ .

**Figure 2b** reports the formation quantum yields of nitrite + HONO ( $\phi_{NO_2^-+HONO}$ ) by the different nitrophenols. The irradiation of 4NP and 2m4NP was quite effective in producing nitrite and HONO. Indeed, the two compounds featured not only the highest  $R_{NO_2^-+HONO}$  formation rates (**Figure 2a**), but also the highest rates per absorbed photon (**Figure 2b**). Both 4NP and 2m4NP in the undissociated form have absorption maxima around 310 nm, with molar absorption coefficients near  $10^4 \text{ M}^{-1} \text{ cm}^{-1}$  (see SI). The values of  $\phi_{NO_2^-+HONO}$  were generally high for the methylated nitrophenols, and quite low for the chlorinated ones. In the case of 4NP,  $\phi_{NO_2^-+HONO}$  was relatively low under basic conditions compared to more acidic pH values, differently from the observed pH trend of  $R_{NO_2^-+HONO}$  (**Figure 2a**). Because  $\phi_{NO_2^-+HONO} = R_{NO_2^-+HONO} (P_a^{NP})^{-1}$ , the reason is the shift toward visible wavelengths of the absorption of 4-nitrophenolate, compared to the undissociated 4-nitrophenol (see **Figure 1**). This fact causes the nitrophenolate to absorb a larger fraction of lamp radiation, and to attain a higher  $P_a^{NP}$  value than the undissociated nitrophenol.

Differently from  $\phi_{NO_2^-+HONO}$ , there are several literature data concerning the direct photolysis quantum yields of nitrophenols ( $\phi_{NP}$ ), which allow a comparison with our results. **Figure 2c** reports  $\phi_{NP}$  for the different nitrophenols and pH conditions under study. All the methylnitrophenols and 4NP had relatively high quantum yields for the direct photolysis, while we observed low quantum yield values for the chloronitroderivatives. In the case of 2NP we obtained  $\phi_{2NP} = (1.1 \pm 0.1) \cdot 10^{-4}$  at the natural pH (~6), which compares well with the value reported in a previous study under comparable pH conditions and simulated sunlight irradiation ( $8.4 \cdot 10^{-5}$ ).<sup>34</sup> Alif et al. have found that  $\phi_{2NP}$  at pH=8.2 varies with the irradiation wavelength, from  $1.3 \cdot 10^{-3}$  at 254 nm to  $2.2 \cdot 10^{-6}$  at 365 nm.<sup>36</sup> The pH conditions used by Alif et al. were intermediate between our natural pH and pH~10, and in the latter case we obtained  $\phi_{2NP} = (7.3 \pm 0.6) \cdot 10^{-6}$ . Not surprisingly given the respective pH

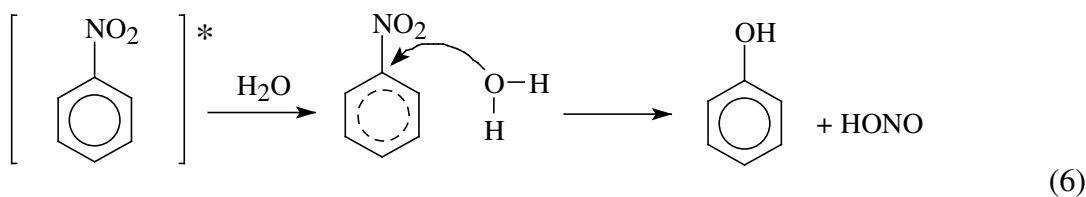
and irradiation conditions, our  $\phi_{2NP}$  values are included into the wide range of quantum yields reported by Alif et al.<sup>36</sup> In the case of 4NP at the natural pH, our value  $\phi_{4NP} = (2.5 \pm 0.2) \cdot 10^{-4}$  compares well with a previous report at pH~6 under simulated sunlight ( $3.3 \cdot 10^{-4}$ ).<sup>34</sup> At pH~3 under simulated sunlight we found  $\phi_{4NP} = (7.3 \pm 0.5) \cdot 10^{-4}$ . Under 210-400 nm broadband irradiation and pH=2.5 it has been reported  $\phi_{4NP} = 4.3 \cdot 10^{-4}$ ,<sup>56</sup> and at pH=2-4 under irradiation at  $\lambda > 290$  nm it has been reported  $\phi_{4NP} = 1.1 \cdot 10^{-4}$ .<sup>57</sup> At 365 nm it has been found  $\phi_{4NP} = (4.5 \pm 0.6) \cdot 10^{-5}$  at pH=2,  $(3.0 \pm 0.6) \cdot 10^{-5}$  at pH=5.5, and  $(1.8 \pm 0.5) \cdot 10^{-5}$  at pH=8.3,<sup>37</sup> but these low values compared to other reports could be caused by the relatively high irradiation wavelength. Overall, it seems that  $\phi_{4NP}$  could vary by a factor of up to ~6 when determined with different experimental set-ups, although under seemingly comparable irradiation wavelengths. This issue should be taken into account when comparing, e.g., our data obtained in aqueous solutions and in viscous systems (flow tubes, *vide infra*).

As far as 24dNP is concerned, our results ( $\phi_{24dNP} = (2.1 \pm 0.1) \cdot 10^{-4}$  at pH~3,  $(1.3 \pm 0.1) \cdot 10^{-4}$  at pH~6 and  $(2.0 \pm 0.3) \cdot 10^{-5}$  at pH~10) were roughly comparable with those obtained under 210-400 nm irradiation at pH=2.5 ( $\phi_{24dNP} = 1.3 \cdot 10^{-4}$ ),<sup>56</sup> and under UVA irradiation at pH=2.4 and pH=7.3 ( $\phi_{24dNP} = (8.1 \pm 0.4) \cdot 10^{-5}$  and  $(3.5 \pm 0.2) \cdot 10^{-5}$ , respectively).<sup>58</sup> In contrast, Lignell et al. reported  $\phi_{24dNP} = 4 \cdot 10^{-6}$  for the direct photolysis of 24dNP in acidified water, under 280-400 nm broadband irradiation.<sup>42</sup> This is at variance with most literature findings, although the calculation of  $\phi_{24dNP}$  in water was not the main goal of Lignell et al. They monitored the time trend of 24dNP by 290 nm single-wavelength absorption spectroscopy<sup>42</sup> and, because the photolysis of 24dNP yields radiation-absorbing compounds,<sup>58</sup> the spectrophotometric monitoring might unfortunately provide an underestimation of the 24dNP transformation rate and, therefore, of the photolysis quantum yield.

The above data suggest that the photolysis quantum yields of nitrophenols depend on both pH and the irradiation wavelength(s). The pH dependence is linked to the occurrence of undissociated nitrophenols and nitrophenolates, involved in acid-base equilibria. The wavelength dependence could be at least partially accounted for by the fact that the UVC photolysis of nitrophenols proceeds by photoionisation,<sup>38</sup> while irradiation at longer wavelengths triggers different photoreaction pathways.<sup>39</sup>

The yield of nitrite+HONO per photolysed nitrophenol molecule ( $\omega_{NO_2^-+HONO}$ , see **Figure 2d**) is also important because different compounds could undergo different photolytic pathways involving the release of nitrite+HONO to different extents. Within each class of substrates (unsubstituted, chlorinated or methylated nitrophenols), the highest values of  $\omega_{NO_2^-+HONO}$  were found for the *para*-nitroisomers (4NP, 26dCl4NP, 2m4NP). The case of 24dNP is peculiar, because this compound has two nitro groups that could theoretically release a double amount of nitrite+HONO compared to the other nitrophenols under study. However, the  $\omega_{NO_2^-+HONO}$  values of 24dNP are very similar to those of 4NP and higher than those of 2NP, which might imply that nitrite+HONO is mostly released by the nitro group in *para* position with respect to the phenolic -OH. Interestingly, Alif et al. found a ~10% yield of nitrite from 4NP in acidic conditions,<sup>37</sup> which is in very good agreement with the  $\omega_{NO_2^-+HONO}$  values of 4NP reported in **Figure 2d**.

There is literature evidence that the release of HONO/NO<sub>2</sub><sup>-</sup> upon direct photolysis of nitroaromatic compounds in aqueous solution takes place *via* a photohydrolysis pathway involving the light-excited nitroaromatic molecule. In this process a water molecule attacks the C-N bond on the side of the ring C atom, as per reaction (6) where the asterisk denotes a light-excited species.<sup>59</sup>



Steric hindrance by nearby substituents could inhibit the interaction of water with the C-N bond, thereby making nitrite release more difficult. Among the studied compounds, the *para*-nitrophenols have the least sterically hindered nitro groups, and it looks reasonable that they feature the easiest release of HONO/NO<sub>2</sub><sup>-</sup> upon irradiation.

***Direct quantification of HONO release from highly viscous organic-water mixtures: A flow tube study***

**Figure 3** reports the formation quantum yields of HONO, derived based on the HONO release rate from the film and on the absorbed photon flux of 4NP in the film. To derive both quantities from the gas-phase HONO mixing ratio and the irradiance at the surface of the flow tube, the volume of the liquid sample in the coated wall flow tube needs to be known. In these experiments, citric acid was used as matrix to define the volume of the liquid samples by equilibrating the water content of the solution with the partial pressure of water in the gas-phase of the flow reactor. At a relative humidity of 74% (21°C), citric acid takes up water until a solution of 10 mol/kg Molality is formed,<sup>60</sup> which corresponds to a viscosity of 4.7·10<sup>-2</sup> Pa s.<sup>61</sup> Based on the total amount of citric acid that was applied to the flow tube (17-158 mg) and on the geometric surface area of 201 cm<sup>2</sup>, a film volume of 29-185 μL can be derived.

This assessment bears some systematic uncertainty for the films where the pH was set to 3 or 7 by adding NaOH. In these mixed NaOH-citric acid-water systems, the equilibrium concentration at given relative humidity is not known, and calculations have been done in this work by assuming

that the water uptake of citric acid - sodium citrate - water systems equals that of citric acid - water systems. To estimate the systematic error based on this assumption for the volume calculation in our work, we repeated the calculation based on the water uptake of sodium citrate extrapolated from the data by Schunk, which give a Molality of 5 mol/kg at equilibrium.<sup>62</sup>

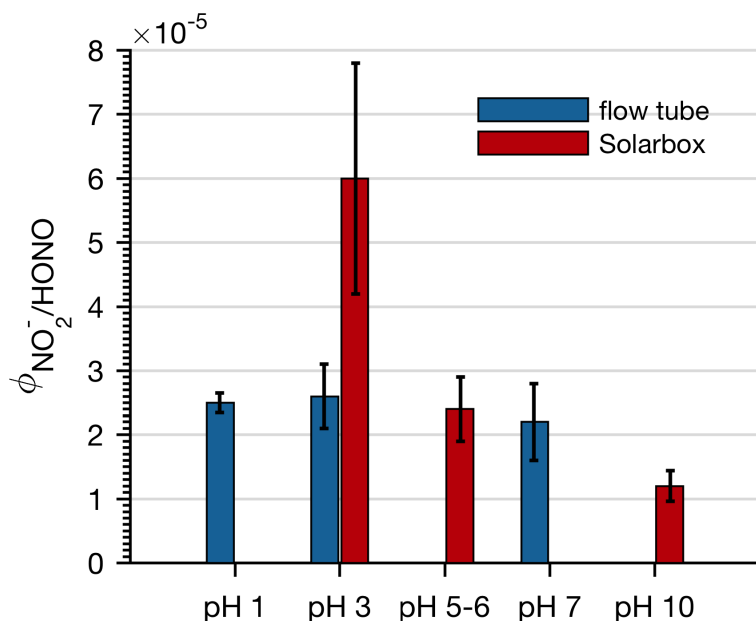


**Figure 3.** Quantum yields for the photochemical production of HONO or  $\text{HONO}/\text{NO}_2^-$  from 4NP at different pH values, in aqueous solution under simulated sunlight in the Solarbox set-up (red bars), and in the flow tube experiments with aqueous citric acid solution (blue bars). Error bars represent standard deviation of repeated experiments.

Based on this assessment, one gets HONO release rates of  $0.8 \cdot 10^{-9} \text{ M s}^{-1}$  at pH=3 and  $1.1 \cdot 10^{-9} \text{ M s}^{-1}$  at pH=7, with respective absorbed photon fluxes by 4NP of  $2.6 \cdot 10^{-5}$  and  $2.2 \cdot 10^{-5} \text{ Ein L}^{-1} \text{ s}^{-1}$  (note that 1 Ein = 1 mole of photons). The uncertainty in volume calculation has no impact on the quantum yield, and the uncertainties in rate and photon flux are not larger than the standard deviation of repeated experiments.

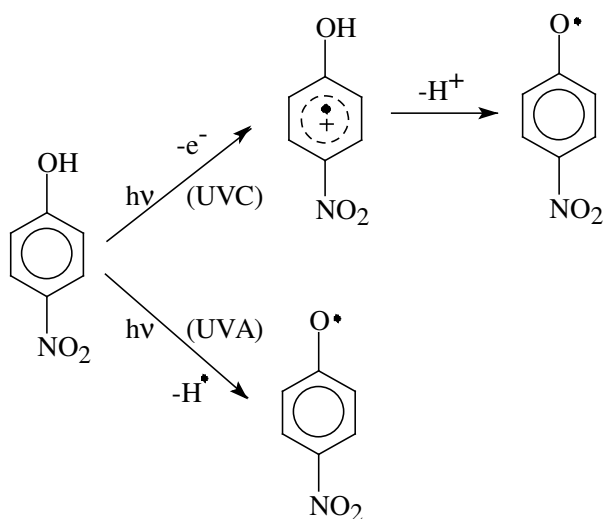
The 4NP experiments in aqueous solution under simulated sunlight (Solarbox) and in the flow tube were carried out under different viscosity and irradiation conditions, which should be taken into account when making a comparison. In particular, as already discussed, the wavelength range of irradiation may be important for the measured photolysis quantum yields of nitrophenols. Moreover, viscous systems favour the recombination of photo-fragments produced in the primary photolysis step, which can potentially influence the photolysis quantum yields.<sup>44,45</sup>

Remarkably similar values of the quantum yields of (nitrite+)HONO production from 4NP ( $\phi_{NO_2/HONO}$ ) were obtained in Solarbox and in the flow tube (**Figure 3**), the largest difference by a factor  $\sim 2$  being observed at pH=3. When considering that literature reports of nitrophenol photodegradation quantum yields under apparently comparable conditions vary by a factor of up to 6 (see previous discussion), the values reported in **Figure 3** can be considered as approximately comparable between the two series of experiments. The overall agreement between results in the water phase and in viscous water-organic mixtures could be explained by the fact that, although different, the emission spectra of both irradiation set-ups overlapped with the absorption spectrum of 4NP between 300 and 450-500 nm (see **Figure 1**). Both lamps would thus excite the same long-wavelength absorption bands of 4NP (either the undissociated compound, or the nitrophenolate when applicable), inducing similar processes with similar quantum yields. The light-driven HONO formation from 4NP photolysis would thus occur in complex matrixes as found in atmospheric aerosol, with about the same overall yield as in diluted aqueous solutions. This finding is in general agreement with Dubowski and Hoffmann,<sup>63</sup> who studied the photochemistry of 4NP in ice and found a quantum yield of 4NP loss of  $2 \cdot 10^{-4}$ , concluding that similar mechanisms are operating in frozen systems and in the liquid water phase. Note that the experiments with viscous citric acid showed a long-term decrease of reactivity, indicating that there might be a strong impact of time on the yield. To extrapolate reactivity in more complex, aged aerosol additional studies are needed.

### *Laser flash photolysis of nitrophenols*

The direct photolysis process plays a key role in the photogeneration of HONO/NO<sub>2</sub><sup>-</sup> by nitrophenols. The transformation pathways that nitrophenols undergo soon after radiation absorption were studied with the laser flash photolysis (LFP) technique, irradiating the samples at 355 nm. The overall results of the LFP of the various nitrophenols under study are shown in the SI. At acidic pH it was observed the formation of a transient species with absorption maximum centred at 390-440 nm, which followed a first-order decay kinetics with rate constant between 10<sup>5</sup> and 10<sup>7</sup> s<sup>-1</sup>. The rate constants were not modified by bubbling Ar into the solution to eliminate dissolved oxygen. This finding suggests that the detected transients are not excited triplet states, which should react efficiently with O<sub>2</sub> to produce <sup>1</sup>O<sub>2</sub>.<sup>64</sup> Based on the observed absorption maxima and on the lack of an oxygen effect, one can identify the transients generated by LFP as the phenoxy radicals of the nitrophenols.<sup>65</sup>

In a previous study, nitrophenols have been photolysed by laser in the UVC region with the detection of phenoxy radicals and solvated electrons. The UVC photolysis of nitrophenols could thus occur by photoionisation, followed by deprotonation of the phenol radical cation to yield the phenoxy radical.<sup>38</sup> In our experiments we found no evidence for the formation of solvated electrons, which would be easily detected in the absence of oxygen due to their prominent absorption maximum at 720 nm.<sup>66</sup> If photoionisation is excluded, the most likely pathway to phenoxy is the homolytic breaking of the phenolic O-H bond with release of a hydrogen atom, which would escape detection because of its low and short-wavelength absorption ( $\lambda < 250$  nm).<sup>67</sup> The two alternative pathways that can yield the phenoxy radical are depicted in reaction (7).



(7)

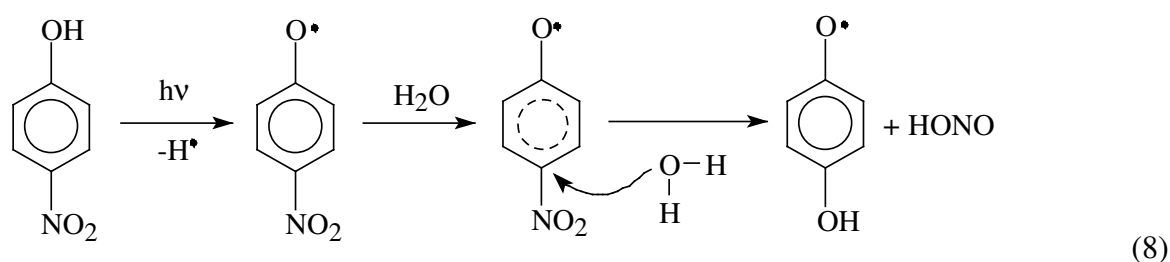
The occurrence of photoinduced phenolic bond homolysis instead of photoionisation has also been observed with other (non nitrated) phenolic compounds, when carrying out LFP experiments in the UVA region.<sup>39</sup> We performed LFP experiments also at alkaline pH values (8 to 10), but it was generally not possible to detect either phenoxy radicals or solvated electrons. There was the single exception of 4Cl<sub>2</sub>NP that yielded a low-intensity signal at pH=8.9, which could be attributed to its phenoxy radical. Therefore, in most cases our study is silent as to the primary photolysis pathways of the nitrophenolates.

By combining literature data concerning the release of the nitro group upon nitroaromatic irradiation<sup>37,59</sup> and the results of the present LFP experiments, one can suppose that the primary step in the case of the undissociated nitrophenols is a bond-breaking process. It involves homolysis of the phenolic O-H bond to yield the corresponding nitrophenoxy radical, PhO•. The release of the nitro group could take place upon reaction between PhO• and water. In a previous study it has been hypothesised a reaction between a water molecule and the light-excited nitroaromatic compound.<sup>59</sup> Our LFP data suggest that, in the case of the undissociated nitrophenols, the most likely "light-excited species" reacting with water are the phenoxy radicals formed upon nitrophenols excitation. Although it is possible that minor photoinduced pathways yield additional excited states, not

detected by LFP, one should consider that the HONO/NO<sub>2</sub><sup>-</sup> yields ( $\omega_{NO_2^-+HONO}$ , see **Figure 1d**) were <1 but far from negligible. This datum hardly supports the hypothesis that HONO/NO<sub>2</sub><sup>-</sup> is produced by a minor photoreaction pathway that does not involve PhO<sup>•</sup>.

### *Environmental implications*

The direct photolysis of nitrophenols under environmentally significant conditions would mainly proceed by O-H bond breaking to give the corresponding phenoxy radicals, which could possibly yield HONO through further reaction with water (see below).



The above reaction scheme was proposed based on experimental data and literature references.<sup>59</sup> However, it should be pointed out that we have no compelling evidence for the nitro group to be directly eliminated as HONO/NO<sub>2</sub><sup>-</sup>. Alternative explanations cannot be excluded such as the elimination of the nitro group as <sup>•</sup>NO<sub>2</sub>, followed by reaction of <sup>•</sup>NO<sub>2</sub> with another phenolic compound to produce a phenoxy radical and HONO/NO<sub>2</sub><sup>-</sup>. Moreover, our steady irradiation experiments were carried out over time scales that are much longer than the phenoxy radical lifetime. Therefore, the nitro group elimination could also involve later reaction intermediates, different from the phenoxy radicals.

The production of HONO/NO<sub>2</sub><sup>-</sup> was most important for the *para*-nitrophenols, probably because of the lower steric hindrance of their nitro group. Interestingly, the methyl-substituted nitrophenols had

higher  $\phi_{NO_2^-+HONO}$  values than the chloro-substituted ones. Given the electron-donating character of the methyl group and the electron-withdrawing character of the chloro one, in the context of reaction (8) it is possible that the water-molecule attack is easier for relatively electron-rich rings.

Previous studies have shown that the gas-phase photolysis of *ortho*-nitrophenols is a potentially important HONO source.<sup>20,21</sup> Here we show that the aqueous-phase photolysis of *para*-nitrophenols may be an additional source of HONO/NO<sub>2</sub><sup>-</sup>. Interestingly, the direct photolysis is an important transformation pathway for nitrophenols in the atmospheric aqueous phase. In the case of 24dNP it has been suggested that direct photolysis and <sup>•</sup>OH reaction are the main photochemical sinks, with comparable importance.<sup>58</sup> Among the aqueous phases in contact with the atmosphere, dew water has shown potential to contribute to the morning levels of atmospheric HONO. In the presence of gas-phase HONO concentrations in the tens pptv range, a gas-phase HONO peak has been observed despite important photolytic loss, at about the same middle-morning time when dew water evaporates.<sup>68,69</sup> Two processes have been suggested to contribute to such an increase in gas-phase HONO, namely (i) release as HONO of the dissolved HONO/NO<sub>2</sub><sup>-</sup> upon dew-water evaporation, and (ii) photolysis of HNO<sub>3</sub> adsorbed on surfaces exposed to the atmosphere.<sup>68,69</sup> Moreover, evidence has been provided that dew evaporation plays a significant role.<sup>69</sup> The occurrence of HONO/NO<sub>2</sub><sup>-</sup> in dew water partially depends on previous HONO dissolution from the gas phase,<sup>19</sup> and it is interesting to see whether nitrophenols have the potential to contribute to the observed HONO/NO<sub>2</sub><sup>-</sup> levels in dew water. The formation yields of HONO/NO<sub>2</sub><sup>-</sup> from irradiated nitrophenols are often around 10% (see **Figure 2d**). Under these circumstances, if the reaction is fast enough (which could be the case for 4NP, 2m4NP and, to a lesser extent, for 24dNP, 4m2NP and 3m2NP), 10<sup>-6</sup> M nitrophenol levels (actually detected in urban atmospheric waters)<sup>31,70,71</sup> under favourable conditions could yield 10<sup>-7</sup> M HONO/NO<sub>2</sub><sup>-</sup>. In highly polluted atmosphere (Santiago, Chile) dissolution of ~10 ppbv gas-phase HONO has been shown to produce dew-water

HONO/NO<sub>2</sub><sup>-</sup> at 10<sup>-4</sup> M concentration,<sup>19</sup> which is around three orders of magnitude higher than the HONO/NO<sub>2</sub><sup>-</sup> concentrations potentially produced by nitrophenol photolysis. However, one should also consider that an important dew-water impact on gas-phase HONO has been observed at atmospheric HONO levels that were about three orders of magnitude lower than in Santiago (tens pptv instead of ~10 ppbv).<sup>19,68,69</sup> The dissolution of gas-phase HONO into dew water cannot be described by a simple Henry's law equilibrium<sup>19</sup> but, by assuming that the aqueous-phase concentration scales with the gas-phase one, dissolution of ten-pptv HONO into dew water might produce 10<sup>-7</sup> M HONO/NO<sub>2</sub><sup>-</sup>. That would be quite comparable to the amount potentially produced by photolysis of 10<sup>-6</sup> M nitrophenols. Nitrophenols in dew water have thus the potential to produce dissolved HONO/NO<sub>2</sub><sup>-</sup> at comparable concentrations as HONO dissolution from the gas phase, under conditions where dew evaporation can impact the morning levels of gas-phase HONO. As a possibly important source of gas-phase HONO, the aqueous photolysis of *para*-nitrophenols requires additional investigation.

The formation rate data reported in **Figure 2a** (and particularly those at the natural pH, which are more common under atmospheric conditions) allow further considerations to be made. The highest formation rate of nitrite was observed in the case of 2m4NP, followed by 4NP. This photochemical behaviour would be compensated for by the higher occurrence of 4NP in the atmosphere: when the two compounds have been simultaneously detected in atmospheric waters, the 4NP:2m4NP concentration ratio was around 3.<sup>72</sup> Furthermore, compounds such as 24dNP, 3m2NP and 4m2NP can reach roughly comparable concentration values in atmospheric waters,<sup>70,71</sup> and they also produce HONO/NO<sub>2</sub><sup>-</sup> with comparable formation rates (**Figure 2a**). Therefore, these compounds could have similar importance as photochemical sources of nitrite and HONO to the atmosphere.

## Acknowledgements

DV, VM and CM acknowledge financial support by MIUR-PNRA. MB and GM acknowledge financial support provided by the CPER (Ministry, Region and FEDER Europe).

## Supporting Information Available

The Supporting Information is available free of charge on the ACS Publications website at DOI: %%%%. It concerns additional analytical details (liquid chromatography separations), absorption spectra, and the detailed results of the laser flash photolysis experiments (PDF).

## References

- (1) Spataro, F.; Ianniello, A. Sources of atmospheric nitrous acid: State of the science, current research needs, and future prospects. *J. Air Waste Manage. Assoc.* **2014**, *64*, 1232-1250.
- (2) Bartolomei, V.; Gomez Alvarez, E.; Wittmer, J.; Tlili, S.; Strekowski, R.; Temime-Roussel, B.; Quivet, E.; Wortham, H.; Zetzsch, C.; Kleffmann, J.; Gligorovski, S. Combustion processes as a source of high levels of indoor hydroxyl radicals through the photolysis of nitrous acid. *Environ. Sci. Technol.* **2015**, *49*, 6599-6607.
- (3) Gomez Alvarez, E.; Amedro, D.; Afif, C.; Gligorovski, S.; Schoemaeker, C.; Fittschen, C.; Doussin, J. F.; Wortham, H. Unexpectedly high indoor hydroxyl radical concentrations associated with nitrous acid. *Proc. Natl. Acad. Sci. U. S. A.* **2013**, *110*, 13294-13299.
- (4) Elshorbany, Y.; Barnes, I.; Becker, K. H.; Kleffmann, J.; Wiesen, P. Sources and cycling of tropospheric hydroxyl radicals - An overview. *Z. Phys. Chemie* **2010**, *224*, 967-987.
- (5) Gligorovski, S.; Strekowski, R.; Barbati, S.; Vione, D. Environmental implications of hydroxyl radicals ( $\bullet\text{OH}$ ). *Chem Rev.* **2015**, *115*, 13051-13092.

- (6) Rohrer, F.; Lu, K.; Hofzumahaus, A.; Bohn, B.; Brauers, T.; Chang, C.-C.; Fuchs, H.; Häseler, R.; Holland, F.; Hu, M.; Kita, K.; Kondo, Y.; Li, X.; Lou, S.; Oebel, A.; Shao, M.; Zeng, L.; Zhu, T.; Zhang, Y.; Wahner, A., Maximum efficiency in the hydroxyl-radical-based self-cleansing of the troposphere. *Nature Geosci.* **2014**, *7*, 559-563.
- (7) Elshorbany, Y. F.; Kurtenbach, R.; Wiesen, P.; Lissi, E.; Rubio, M.; Villena, G.; Gramsch, E.; Rickard, A. R.; Pilling, M. J.; Kleffmann, J. Oxidation capacity of the city air of Santiago, Chile. *Atmos. Chem. Phys.* **2009**, *9*, 2257-2273.
- (8) Calvert, J. G.; Yarwood, G.; Dunker, A. M. An evaluation of the mechanism of nitrous-acid formation in the urban atmosphere. *Res. Chem. Interim.* **1994**, *20*, 463-502.
- (9) Wu, D. M.; Kampf, C. J.; Pöschl, U.; Oswald, R.; Cui, J.; Ermel, M.; Hu, C.; Trebs, I.; Sörgel, M. Novel tracer method to measure isotopic labeled gas-phase nitrous acid (HONO-<sup>15</sup>N) in biogeochemical studies. *Environ. Sci. Technol.* **2014**, *48*, 8021-8027.
- (10) Lee, J. D.; Whalley, L. K.; Heard, D. E.; Stone, D.; Dunmore, R. E.; Hamilton, J. F.; Young, D. E.; Allan, J. D.; Laufs, S.; Kleffmann, J. Detailed budget analysis of HONO in central London reveals a missing daytime source. *Atmos. Chem. Phys.* **2016**, *16*, 2747-2764.
- (11) George, C.; Ammann, M.; D'Anna, B.; Donaldson, D. J.; Nizkorodov, S. A. Heterogeneous photochemistry in the atmosphere. *Chem. Rev.* **2015**, *115*, 4218-4258.
- (12) Ma, J.; Liu, Y.; Han, C.; Ma, Q.; Liu, C.; He, H. Review of heterogeneous photochemical reactions of NO<sub>y</sub> on aerosol - A possible daytime source of nitrous acid (HONO) in the atmosphere. *J. Environ. Sci.* **2013**, *25*, 326-334.
- (13) Ammar, R.; Monge, M. E.; George, C.; D'Anna, B. Photoenhanced NO<sub>2</sub> loss on simulated urban grime. *ChemPhysChem* **2010**, *11*, 3956-3961.
- (14) Stemmler, K.; Ammann, M.; Donders, C.; Kleffmann, J.; George, C. Photosensitized reduction of nitrogen dioxide on humic acid as a source of nitrous acid. *Nature* **2006**, *440*, 195-198.

- (15) Su, H.; Cheng, Y.; Oswald, R.; Behrendt, T.; Trebs, I.; Meixner, F. X.; Andreae, M. O.; Cheng, P.; Zhang, Y.; Pöschl, U. Soil nitrite as a source of atmospheric HONO and OH radicals. *Science* **2011**, *333*, 1616-1618.
- (16) Oswald, R.; Behrendt, T.; Ermel, M.; Wu, D.; Su, H.; Cheng, Y.; Breuninger, C.; Moravek, A.; Mougín, E.; Delon, C.; Loubet, B.; Pommerening-Röser, A.; Sörgel, M.; Pöschl, U.; Hoffmann, T.; Andreae, M. O.; Meixner, F. X.; Trebs, I. HONO emissions from soil bacteria as a major source of atmospheric reactive nitrogen. *Science* **2013**, *341*, 1233-1235.
- (17) Acker, K.; Beysens, D.; Möller, D. Nitrite in dew, fog, cloud and rain water: An indicator for heterogeneous processes on surfaces. *Atmos. Res.* **2008**, *87*, 200-212.
- (18) Rubio, M. A.; Lissi, E.; Villena, G. Factors determining the concentration of nitrite in dew from Santiago, Chile. *Atmos. Environ.* **2008**, *42*, 7651-7656.
- (19) Rubio, M. A.; Lissi, E.; Villena, G.; Elshorbany, Y. F.; Kleffmann, J.; Kurtenbach, R.; Wiesen, P. Simultaneous measurements of formaldehyde and nitrous acid in dews and gas phase in the atmosphere of Santiago, Chile. *Atmos. Environ.* **2009**, *43*, 6106-6109.
- (20) Bejan, I.; Abd El Aal, Y.; Barnes, I.; Benter, T.; Bohn, B.; Wiesen, P.; Kleffmann, J. The photolysis of ortho-nitrophenols: a new gas phase source of HONO. *Phys. Chem. Chem. Phys.* **2006**, *8*, 2028-2035.
- (21) Chen, J.; Wenger, J. C.; Venables, D. S. Near-ultraviolet absorption cross sections of nitrophenols and their potential influence on tropospheric oxidation capacity. *J. Phys. Chem. A* **2011**, *115*, 12235-12242.
- (22) Rippen, G.; Zietz, E.; Frank, R.; Knacker, T.; Klöpffer, W. Do airborne nitrophenols contribute to forest decline? *Environ. Technol. Lett.* **1987**, *8*, 475-482.
- (23) Natangelo, M.; Mangiapan, S.; Bagnati, R.; Benfenati, E.; Fanelli, R. Increased concentrations of nitrophenols in leaves from a damaged forestal site. *Chemosphere* **1999**, *38*, 1495-1503.

- (24) Luttke, J.; Scheer, V.; Levsen, K.; Wunsch, G.; Cape, J. N.; Hargreaves, K. J.; Storeton-West, R. L.; Acker, K.; Wieprecht, W.; Jones, B. Occurrence and formation of nitrated phenols in and out of cloud. *Atmos. Environ.* **1997**, *31*, 2637-2648.
- (25) Heal, M. R.; Harrison, M. A. J.; Cape, J. N. Aqueous-phase nitration of phenol by  $N_2O_5$  and  $ClNO_2$ . *Atmos. Environ.* **2007**, *41*, 3515-3520.
- (26) Kroflic, A.; Grilc, M.; Grgic, I. Does toxicity of aromatic pollutants increase under remote atmospheric conditions? *Sci. Rep.* **2015**, *5*, 8859.
- (27) Kroflic, A.; Grilc, M.; Grgic, I. Unraveling pathways of guaiacol nitration in atmospheric waters: Nitrite, a source of reactive nitronium ion in the atmosphere. *Environ. Sci. Technol.* **2015**, *49*, 9150-9158.
- (28) Perrone, M. G.; Carbone, C.; Faedo, D.; Ferrero, L.; Maggioni, A.; Sangiorgi, G.; Bolzacchini, E. Exhaust emissions of polycyclic aromatic hydrocarbons, n-alkanes and phenols from vehicles coming within different European classes. *Atmos. Environ.* **2014**, *82*, 391-400.
- (29) Vione, D.; Maurino, V.; Minero, C.; Pelizzetti, E. Aqueous atmospheric chemistry: Formation of 2,4-dinitrophenol upon nitration of 2-nitrophenol and 4-nitrophenol in solution. *Environ. Sci. Technol.* **2005**, *39*, 7921-7931.
- (30) Harrison, M. A. J. ; Barra, S.; Borghesi, D.; Vione, D.; Arsene, C.; Olariu, R. I. Nitrated phenols in the atmosphere: a review. *Atmos. Environ.* **2005**, *39*, 231-248.
- (31) Rubio, M. A.; Lissi, E.; Herrera, N.; Perez, V.; Fuentes, N. Phenol and nitrophenols in the air and dew waters of Santiago de Chile. *Chemosphere* **2012**, *86*, 1035-1039.
- (32) Aptula, A. O.; Netzeva, T. I.; Valkova, I. V.; Cronin, M. T. D.; Schultz, T. W.; Kühne, R.; Schüürmann, G. Multivariate discrimination between modes of toxic action of phenols. *Quant. Struct-Act. Relat.* **2002**, *21*, 12-22.
- (33) Harrison, M. A. J.; Cape, J. N.; Heal, M. R. Experimentally determined Henry's Law coefficients of phenol, 2-methylphenol and 2-nitrophenol in the temperature range 281-302 K. *Atmos. Environ.* **2002**, *36*, 1843-1851.

- (34) Vione, D.; Maurino, V.; Minero, C.; Duncianu, M.; Olariu, R. I.; Arsene, C.; Sarakha, M.; Mailhot, G. Assessing the transformation kinetics of 2- and 4-nitrophenol in the atmospheric aqueous phase. Implications for the distribution of both nitroisomers in the atmosphere. *Atmos. Environ.* **2009**, *43*, 2321-2327.
- (35) Hinrichs, R. Z.; Buczek, P.; Trivedi, J. J. Solar absorption by aerosol-bound nitrophenols compared to aqueous and gaseous nitrophenols. *Environ. Sci. Technol.* **2016**, *50*, 5661-5667.
- (36) Alif, A.; Pilichowski, J. F.; Boule, P. Photochemistry and environment XIII: Phototransformation of 2-nitrophenol in aqueous solution. *J. Photochem. Photobiol. A: Chem.* **1991**, *59*, 209-219.
- (37) Alif, A.; Boule, P.; Lemaire, J. Comportement photochimique du nitro-4-phenol en solution aqueuse. *Chemosphere* **1987**, *16*, 2213-2223.
- (38) Zhao, S.; Ma, H. J.; Wang, M.; Cao, C. Q.; Xiong, J.; Xu, Y.; Yao, S. Study on the mechanism of photo-degradation of p-nitrophenol exposed to 254 nm UV light. *J. Haz. Mat.* **2010**, *180*, 86-90.
- (39) De Laurentiis, E.; Minella, M.; Sarakha, M.; Marrese, A.; Minero, C.; Mailhot, G.; Brigante, M.; Vione, D. Photochemical processes involving the UV absorber benzophenone-4 (2-hydroxy-4-methoxybenzophenone-5-sulphonic acid) in aqueous solution: Reaction pathways and implications for surface waters. *Water Res.* **2013**, *47*, 5943-5953.
- (40) Anastasio, C.; Chu, L. Photochemistry of nitrous acid (HONO) and nitrous acidium ion ( $\text{H}_2\text{ONO}^+$ ) in aqueous solution and ice. *Environ. Sci. Technol.* **2009**, *43*, 1108-1114.
- (41) Bartels-Rausch, T.; Jacobi, H.-W.; Kahan, T. F.; Thomas, J. L.; Thomson, E. S.; Abbatt, J. P. D.; Ammann, M.; Blackford, J. R.; Bluhm, H.; Boxe, C. S.; Dominé, F.; Frey, M. M.; Gladich, I.; Guzman, M. I.; Heger, D.; Huthwelker, T.; Klan, P.; Kuhs, W. F.; Kuo, M. H.; Maus, S.; Moussa, S. G.; McNeill, V. F.; Newberg, J. T.; Pettersson, J. B. C.; Roeselova, M.; Sodeau, J. R. A review of air-ice chemical and physical interactions (AICI): liquids, quasi-liquids, and solids in snow. *Atmos. Chem. Phys.* **2014**, *14*, 1587-1633.

- (42) Lignell, A.; Hinks, M. L.; Nizkorodov, S. A. Exploring matrix effects on photochemistry of organic aerosols. *Proc. Natl. Acad. Sci. USA* **2014**, *111*, 13780-13785.
- (43) Chu, L.; Anastasio, C. Formation of hydroxyl radical from the photolysis of frozen hydrogen peroxide. *J. Phys. Chem. A* **2005**, *109*, 6264-6271.
- (44) P. Nissenon, D. Dabdub, R. Das, V. Maurino, C. Minero, D. Vione. Evidence of the water-cage effect on the photolysis of  $\text{NO}_3^-$  and  $\text{FeOH}^{2+}$ . Implications of this effect and of  $\text{H}_2\text{O}_2$  surface accumulation on photochemistry at the air-water interface of atmospheric droplets. *Atmos. Environ.* **2010**, *44*, 4859-4866.
- (45) Khudyakov, I.; Levin, P.; Kuzmin, V. Kinetics of geminate recombination of organic free radicals in viscous solvents. *Photochem. Photobiol. Sci.* **2008**, *7*, 1540-1543.
- (46) Martell, A. E.; Smith, R. M. *Critical Stability Constants*, Vol. 1, Plenum Press, New York, 1989.
- (47) Deguillaume, L.; Charbouillot, T.; Joly, M.; Vaïtilingom, M.; Parazols, M.; Marinoni, A.; Amato, P.; Delort, A. M.; Vinateier, V.; Flossmann, A.; Chaumerliac, N.; Pichon, J. M.; Houdier, S.; Laj, P.; Sellegri, K.; Colomb, A.; Brigante, M.; Mailhot, G. Classification of clouds sampled at the puy de Dôme (France) based on 10 years of monitoring of their physicochemical properties. *Atmos. Chem. Phys.* **2014**, *14*, 1485-1506.
- (48) Zhou, X. L.; Qiao, H. C.; Deng, G. H.; Civerolo, K. A method for the measurement of atmospheric HONO based on DNPH derivatization and HPLC analysis. *Environ. Sci. Technol.* **1999**, *33*, 3672-3679.
- (49) De Laurentiis, E.; Minella, M.; Berto, S.; Maurino, V.; Minero, C.; Vione, D. The fate of nitrogen upon nitrite irradiation: Formation of dissolved vs. gas-phase species. *J. Photochem. Photobiol. A: Chem.* **2015**, *307*, 30-34.
- (50) Abbatt, J. P. D. Interactions of atmospheric trace gases with ice surfaces: Adsorption and reaction. *Chem. Rev.* **2003**, *103*, 4783-4800.

- (51) Hofzumahaus, A.; Kraus, A.; Muller, M. Solar actinic flux spectroradiometry: A technique for measuring photolysis frequencies in the atmosphere. *Appl. Optics* **1999**, *38*, 4443-4460.
- (52) Heland, J.; Kleffmann, J.; Kurtenbach, R.; Wiesen, P. A new instrument to measure gaseous nitrous acid (HONO) in the atmosphere. *Environ. Sci. Technol.* **2001**, *35*, 3207-3212.
- (53) Kleffmann, J.; Heland, J.; Kurtenbach, R.; Lorzer, J.; Wiesen, P. A new instrument (LOPAP) for the detection of nitrous acid (HONO). *Environ. Sci. Pollut. Res.* **2002**, *9*, 48-54.
- (54) Bartels-Rausch, T.; Brigante, M.; Elshorbany, Y. F.; Ammann, M.; D'Anna, B.; George, C.; Stemmler, K.; Ndour, M.; Kleffmann, J., Humic acid in ice: Photo-enhanced conversion of nitrogen dioxide into nitrous acid. *Atmos. Environ.* **2010**, *44*, 5443-5450.
- (55) Brigante, M.; Charbouillot, T.; Vione, D.; Mailhot, G. Photochemistry of 1-nitronaphthalene: a potential source of singlet oxygen and radical species in atmospheric waters. *J. Phys. Chem. A* **2010**, *114*, 2830-2836
- (56) García Einschlag, F. S.; Carlos, L.; Capparelli, A. L.; Nraun, A. M.; Oliveros, E. Degradation of nitroaromatic compounds by the UV-H<sub>2</sub>O<sub>2</sub> process using polychromatic radiation sources. *Photochem. Photobiol. Sci.* **2002**, *1*, 520-525.
- (57) Lemaire, J.; Guth, J. A.; Klais, O.; Leahey, J.; Merz, W.; Philp, J.; Wilmes, R.; Wolff, C. J. M. Ring test of a method for assessing the phototransformation of chemicals in water. *Chemosphere* **1985**, *14*, 53-77.
- (58) Albinet, A.; Minero, C.; Vione, D. Phototransformation processes of 2,4-dinitrophenol, relevant to atmospheric water droplets. *Chemosphere* **2010**, *80*, 753-758.
- (59) Chen, B.; Yang, C.; Goh, N. K. Direct photolysis of nitroaromatic compounds in aqueous solutions. *J. Environ. Sci.* **2005**, *17*, 598-604.
- (60) Lienhard, D. M.; Bones, D. L.; Zuend, A.; Krieger, U. K.; Reid, J. P.; Peter, T. Measurements of thermodynamic and optical properties of selected aqueous organic and organic-inorganic mixtures of atmospheric relevance. *J. Phys. Chem. A* **2012**, *116*, 9954-9968.

- (61) Zardini, A. A.; Sjogren, S.; Marcolli, C.; Krieger, U. K.; Gysel, M.; Weingartner, E.; Baltensperger, U.; Peter, T. A combined particle trap/HTDMA hygroscopicity study of mixed inorganic/organic aerosol particles. *Atmos. Chem. Phys.* **2008**, *8*, 5589-5601.
- (62) Schunk, A.; Maurer, G. Activity of water in aqueous solutions of sodium citrate and in aqueous solutions of (an inorganic salt and citric acid) at 298.15 K. *J. Chem. Eng. Data* **2004**, *49*, 944-949.
- (63) Dubowski, Y.; Hoffmann, M. R. Photochemical transformations in ice: Implications for the fate of chemical species. *Geophys. Res. Lett.* **2000**, *27*, 3321-3324.
- (64) Wilkinson, F.; Helman, W. P.; Ross, A. B. Quantum yields for the photosensitized formation of the lowest electronically excited singlet state of molecular oxygen in solution. *J. Phys. Chem. Ref. Data* **1993**, *22*, 113-262.
- (65) Gadosy, T. A.; Shukla, D.; Johnston, L. J. Generation, characterization and deprotonation of phenol radical cations. *J. Phys. Chem. A* **1999**, *103*, 8834-8839.
- (66) Jou, F. Y.; Freeman, G. R. 1977. Shapes of optical spectra of solvated electrons. Effect of pressure. *J. Phys. Chem.* **1977**, *81*, 909-915.
- (67) Nielsen, S.O.; Michael, B. D.; Hart, E. J. Ultraviolet absorption spectra of hydrated electrons, hydrogen, hydroxyl, deuterium, and hydroxyl-d radicals from pulse radiolysis of aqueous solutions. *J. Phys. Chem.*, **1976**, *80*, 2482-248.
- (68) Zhou, X.; Civerolo, K.; Dai, H.; Huang, G.; Schwab, J.; Demerjian, K. Summertime nitrous acid chemistry in the atmospheric boundary layer at a rural site in New York State. *J. Geophys. Res.* **2002**, *107(D21)*, 4590.
- (69) He, Y.; Zhou, X.; Hou, J.; Gao, H.; Bertman, S. B. Importance of dew in controlling the air-surface exchange of HONO in rural forested environments. *Geophys. Res. Lett.* **2006**, *33*, L02813.

- (70) Schummer, C.; Groff, C.; Al Chami, J.; Jaber, F.; Millet, M. Analysis of phenols and nitrophenols in rainwater collected simultaneously on an urban and rural site in east of France. *Sci. Total Environ.* **2009**, *407*, 5637-5643.
- (71) Delhomme, O.; Morville, S.; Millet, M. Seasonal and diurnal variations of atmospheric concentrations of phenols and nitrophenols measured in the Strasbourg area, France. *Atmos. Pollut. Res.* **2010**, *1*, 16-22.
- (72) Ganranoo, L.; Mishra, S. K.; Azad, A. K.; Shigihara, A.; Dasgupta, P. K.; Breitbach, Z. S.; Armstrong, D. W.; Grudpan, K.; Rappenglueck, B. Measurement of nitrophenols in rain and air by two-dimensional liquid chromatography-chemically active liquid core waveguide spectrometry. *Anal. Chem.* **2010**, *82*, 5838-5843.